



# Methodology for fifth generation district heating and cooling network simulation

Charlie Pr Étot, Nicolas Lamaison

## ► To cite this version:

Charlie Pr Étot, Nicolas Lamaison. Methodology for fifth generation district heating and cooling network simulation. ISEC 2024 - International Sustainable Energy Conference 2024, Apr 2024, Graz, Austria. <10.52825/isec.v1i.1123>. <hal-04770762>

**HAL Id: hal-04770762**

**<https://hal.science/hal-04770762v1>**

Submitted on 7 Nov 2024



**HAL** is a multi-disciplinary open access archive for the deposit and dissemination of scientific research documents, whether they are published or not. The documents may come from teaching and research institutions in France or abroad, or from public or private research centers.

L'archive ouverte pluridisciplinaire **HAL**, est destinée au dépôt et à la diffusion de documents scientifiques de niveau recherche, publiés ou non, émanant des établissements d'enseignement et de recherche français ou étrangers, des laboratoires publics ou privés.



Distributed under a Creative Commons CC BY 4.0 - Attribution - International License

# Methodology for 5<sup>th</sup> generation district heating and cooling network simulation

Charlie Prétot<sup>1</sup> , and  
Nicolas Lamaison<sup>1</sup> 

<sup>1</sup>CEA - LITEN, Grenoble, France

\*Correspondence: Charlie Prétot, [charlie.pretot@cea.fr](mailto:charlie.pretot@cea.fr)

**Abstract:** 5<sup>th</sup> generation district heating and cooling networks (5GDHC) will play a role in the reduction of CO<sub>2</sub> emissions and the resilience to global warming. Our analysis of the literature points out that no simulation study proposes a comprehensive enough description of such networks. The simulation solution presented in this article considers the intertwined influences between the thermal-hydraulic balance in the network, the behavior of the decentralized heat pumps and chillers at substations, and the thermal coupling with the ground. For a given simulation scenario, the 3 developed models are iteratively solved until convergence is reached. After showing how the latter is handled, we exhibit an original result about the influence of the differential pressure between the hot and cold pipes.

**Keywords:** 5GDHC, District heating, District cooling, Decentralized Heat pumps

## 1 Introduction

### 1.1 Context

Due to their inherent ability to integrate renewable and waste energies efficiently, urban thermal networks are key systems for any policies aiming at limiting global warming [1]. With the increase in space cooling demands, expected to be multiplied by 1.6 from 2016 to 2050 in Europe [2], urban areas energy systems must evolve. Even though individual reversible heat pumps present some advantages such as modularity and resilience to variations of heat to cold demand ratio, a generalization of their development induces numerous issues: low efficiency of air as thermodynamic source, increased stress on the electrical grid, enhancement of urban heat island phenomenon, architectural integration, etc. In this context and in the frame of smart energy systems development, i.e. systems taking advantage of positive synergies between energy carriers, the concept of 5<sup>th</sup> generation district heating and cooling (5GDHC) systems has been introduced [3]. 5GDHC systems are able to ensure heat and cold demands with high spatial and temporal variability by making use of a set of hydraulic pumps and a network operating close to ambient temperature, which offers a high quality thermodynamic source to a set of distributed thermodynamic machines (heat pumps and/or chillers).

## 1.2 State of the art

The interest in 5GDHC systems has grown significantly over the last 10 years. Throughout Europe, Buffa et. al [3] listed 40 systems in operation. The author highlighted the diversity of both the design and operation principles. They ended up with an interesting classification of the network types, accounting for the number of pipes, the bidirectionalities of flows and energy and the origin of the heat. Sommer et al. [4] classified 5GDHC networks into 3 main categories. First, classical networks are composed of a supply pipe and a return pipe, similarly to older generations networks. Then, bidirectional networks are composed of a hot pipe and a cold pipe, alternatively supply or return pipe depending on the demand in the substations (cold or hot demand). Finally, reservoir networks are composed of only one pipe in which mixing occurs. More recently, Gjoka reviewed the different scientific publications on 5GDHC, distinguishing simulation works from optimisation works [5].

**Table 1.** Main studies with simulations of low temperature networks. The grades symbolize the level of faithfulness according to the authors from 1 (poor description) to 5 (faithful description).

Reference	Thermal description of the substation	Hydraulic description of the network	Thermal losses of the network
Hirsch and Nicolai [6]	2	4	3
Abbugabara et al. [7]	5	3	1
Toffanin et al. [8]	5	3	3
B��nning et al. [9]	5	3	3
Adihou et al. [10]	5	3	4
Maccarini et al. [11]	5	3	5
Saini et al. [12]	3	4	3

Regarding simulation studies, we found 7 different model descriptions in the literature. Hirsch and Nicolai [6] have implemented a thermal hydraulic simulation solution focused on the distribution network. In another study, Abbugabara et al. [7] developed a comprehensive Modelica model of a 5GDHC substation, aiming to compare the utilization of a chiller with that of a direct cooling exchanger. Then, the impact of a 5GDHC network on the flexibility of the electrical grid has been investigated by Toffanin et al. [8]. B  nning et al. [9] demonstrated that the strategy of free-floating temperature yields poorer performances compared to a strategy imposing the balancing plant exit temperatures. In addition, Adihou et al. [10] employed an exergetic approach to evaluate the efficiency of low-temperature networks. The influence of the secondary distribution temperature on network performance has been highlighted by Maccarini et al. [11]. Lastly, Saini et al. [12] utilized Monte Carlo methods coupled with a 5GDHC simulator to assess the sensitivity of the levelized cost of heating (LCOH) to variations in capital expenditures (CAPEX).

Based on our analysis of these different studies, we identify three main points to faithfully describe a 5GDHC network. First, the substation can deliver either cold or heat. The coefficient of performance for the heat pump and the chiller must be described dependant on the temperature of the primary and secondary loops. Then, the network hydraulic description should take into account pressure drop and allow for bidirectional flows with decentralized hydraulic pumps. Finally, one should take into properly the thermal losses whether the pipes are insulated or not. Indeed, there is no consensus whether the pipes have to be insulated or not. Wirtz et al. [13] use non insulated plastic pipes whereas Saini et al. [12] or B  nning et al. [9] use classical pre-insulated pipes.

Table 1 evaluates these three key points in the seven simulations that we previously listed. We observe that no article manage to comprehensively describe the three identified key points.

### 1.3 Main contribution and paper organisation

Based on the analysis of the literature, we concluded that the different modeling solutions were not complete. In the present paper, we aim to develop a versatile 5GDHC simulator describing properly the substation, the hydraulic and the heat losses of the network. In order to do so, the remaining of the paper is organised as follows:

- Section 2 presents the complete model based on the iteration between i) a detailed substation model accounting for temperature dependency, ii) a state-of-the-art thermohydraulic model of the network and iii) a thermal model of the soil to account for heat diffusion in the ground.
- Section 3 introduces a simple case study, used to specifically detail the convergence process between the different models and present a preliminary interesting analysis of the pressure field in such a network.
- Section 4 concludes the paper and presents the perspectives.

## 2 Overall model description

Our solution of simulation is based on three interconnected submodels (substation and consumer, main plant and network, ground). Sections 2.1 to 2.3 present each submodel and section 2.4 presents the iterative process between these submodels.

### 2.1 Substation and Consumer model

The demand is divided in two categories with cooling load denoted  $\dot{Q}_{c,consumer}$  and heating load denoted  $\dot{Q}_{h,consumer}$  (space heating + domestic hot water). These two quantities are positive. The heat load curves of the different buildings are generated thanks to the nPro tool [14], and hypothesis are made regarding the secondary networks temperature, depending on external temperature.

The architecture of the substation is presented in Figure 1. The secondary heating network is supplied by a heat pump and the secondary cooling network is fed by a chiller. The evaporator of the heat pump is connected to the condenser of the chiller. This architecture is consistent with former modeling of 5GDHC networks [15], [16]. Following the imbalance between hot and cold demand, the substation can withdraw (dark red arrows) / rejects (dark blue arrows) heat from / in the network. We assume that both heat pump and chiller are equipped with a variable speed controller allowing to cover 0 to 100 % of the nominal speed.

The coefficients of performance (COP) of both heat pump and chiller are calculated as a fraction  $\eta_{Carnot}$  of the ideal COP of Carnot. Carnot's COP applies on the temperature of the refrigerant in the internal loop. Like B  nning et al. [9], we assume a difference of temperature of  $\Delta T_r = 2^\circ C$  between the outlet water temperature and the refrigerant at both sides of the heat pump / chiller. The heat exchanges between the heat pump and the network, and between the chiller and the network are thus calculated using Equations 1 and 2.

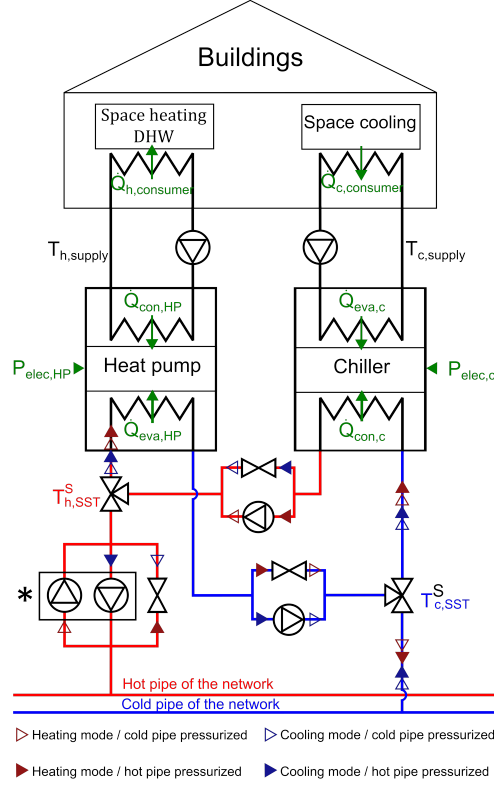


**Figure 1.** Architecture of the substation. The heat is delivered by a heat pump and the chiller delivers the cold. The four different arrows symbolizes the four possible configuration of pressure and demand. For the sake of clarity, different pumps have been drawn depending on the operation modes. In reality one pump in the box \* associated to the proper set of valves may be sufficient.

$$\dot{Q}_{eva,HP} = \dot{Q}_{hot,consumer} \left( 1 - \frac{(T_{h,supply} + \Delta T_r) - (T_{c,SST}^S - \Delta T_r)}{\eta_{Carnot}(T_{h,supply} + \Delta T_r)} \right) \quad (1)$$

$$\dot{Q}_{con,C} = -\dot{Q}_{cold,consumer} \left( 1 + \frac{(T_{h,SST}^S + \Delta T_r) - (T_{c,supply} - \Delta T_r)}{\eta_{Carnot}(T_{c,supply} - \Delta T_r)} \right) \quad (2)$$

Let  $\dot{Q}_{SST}$  be the net exchange of heat between the network and the substation :  $\dot{Q}_{SST} = \dot{Q}_{eva,HP} + \dot{Q}_{con,C}$ . We are able to compute the heat exchange between the network and the substation. Then, we can compute the mass flow rate through the substation using Equation 3.

$$\dot{m}_{SST} = \frac{\dot{Q}_{SST}}{c_P \Delta T_{SST}} \quad (3)$$

$\Delta T_{SST} = T_{h,SST}^S - T_{c,SST}^S$  is the difference of temperature between the outlet and the inlet of the chiller's condenser and between the inlet and the outlet of the heat pump's evaporator. In the general case, each substation has its own  $\Delta T_{SST}$  imposed by the manufacturer of the thermodynamic machine. If  $\dot{m}_{SST} > 0$ , the substation withdraws heat from the network ( $\dot{Q}_{eva,HP} > |\dot{Q}_{con,C}|$ ). If  $\dot{m}_{SST} < 0$ , the substation rejects heat into the network. This mass flow rate is imposed thanks to a control valve or an hydraulic pump (see Figure 1), depending on the dominating demand and the local pressure difference between hot and cold pipe (positive or negative).

## 2.2 Network and Plant model

Knowing the mass flow rate at each substation (see section 2.1) and the thermal losses in each pipe (see section 2.3), we can perform the simulation of the model of network. We use the software DistrictLab-H [17]–[19]. DistrictLab-H is a scalable thermal-hydraulic modeling framework for dynamic simulation of small to large-scale networks. The global thermal-hydraulic model is computed relying on the iteration between a static non-linear hydraulic solver and a dynamic quasi-linear temperature transport solver. The versatility of the tool allows the modeling of the bidirectionality inherent to the type of 5GDHC network here modelled.

There is one pump in each substation and one pump in the main plant. Each pump is in parallel with a control valve (see Figure 1). Following the direction of the flow, the waters goes either through the pump or through the valve.

Thanks to the model of the substation (section 2.1), the heat exchange and the mass flow rate are imposed in each substation of the network.

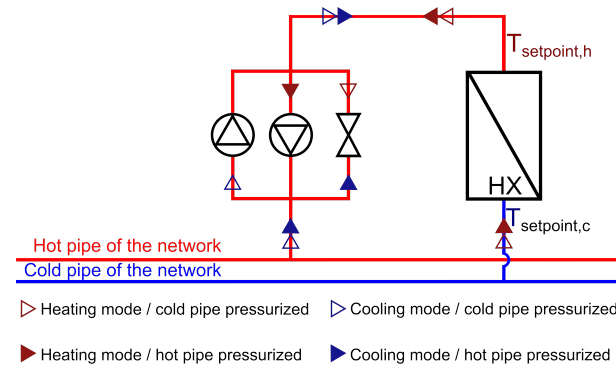


**Figure 2.** Architecture of the main plant. The arrows represent the different configuration. Following the direction of the flow, the heat exchanger controls the hot temperature (heating mode) or the cold temperature (cooling mode).

As shown in Figure 2, the main plant must allow the proper functioning of the network. It imposes a given temperature (temperature of the cold pipe if the cold demand is higher and of the hot pipe in the other case). During post processing, we calculate the cost of the main plant operation from the heat transfer in the central heat exchanger (see Figure 2). This calculation depends on the energy source of the main plant. It is not necessary to impose the flow rate in the main plant (it is imposed by the mass conservation).

## 2.3 Ground model

Figure 3 presents the modeling of the thermal losses for ground buried pipes. From the center towards outside, Figure 3 illustrates the fluid, the pipe wall, the insulation layer, the soil at variable temperature and the undisturbed soil. The description of the thermal transfer in the pipe and the insulation layer ( $R_{fw}$ ,  $C_w$ ,  $R_i$ ) are similar to [18]. In case of uninsulated pipe, we take  $R_i = 0$ . In the latter case, the influence of the fluid temperature on the surrounding ground temperature is enhanced and must be accounted for. Following the work of Maccarini et al. [11], we model the heat transfer in a disk of soil around the pipe (dark brown in Figure 3) thanks to a radial 1D heat conduction equation axisymmetric:

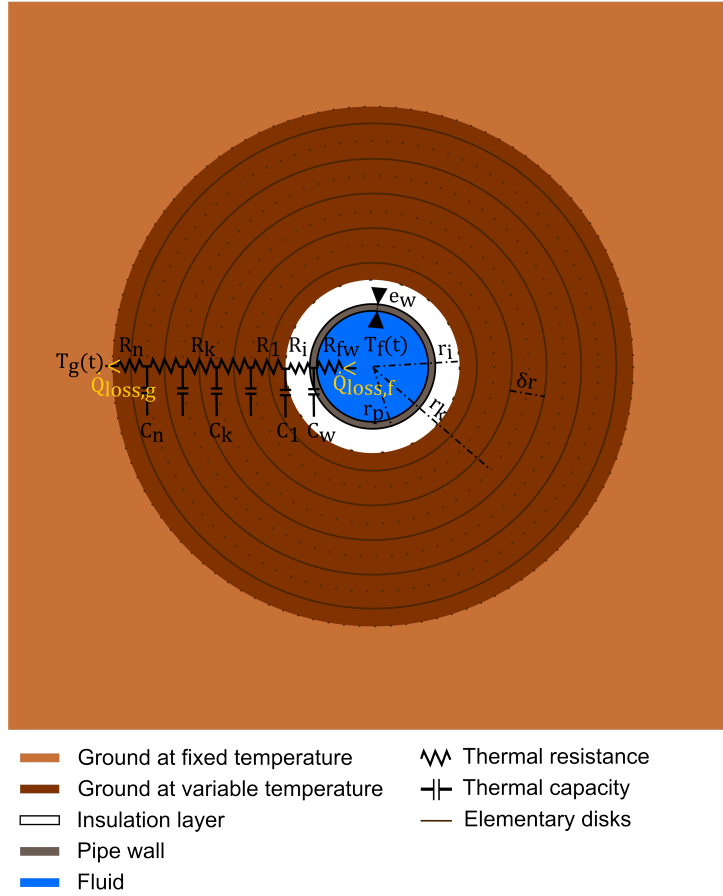


**Figure 3.** Model of thermal losses. Thermal capacities of pipe wall and soil are taken into account. We consider the thermal resistance of the convective heat transfer, the insulation layer and the soil. We must spatially discretize the soil in elementary disks to solve the heat equation.

$$\rho_s c_s \frac{\partial T}{\partial t} = \lambda_s \left( \frac{\partial^2 T}{\partial r^2} + \frac{1}{r} \frac{\partial T}{\partial r} \right), \quad (4)$$

where  $\rho_s$  is the density,  $c_s$  the thermal capacity, and  $\lambda_s$  the thermal conductivity of the soil. There are 2 spatial boundary conditions : the fluid temperature and the undisturbed soil temperature (see Figure 3). There is no analytical solution of Equation 4 for time-dependant spatial boundary conditions. For this reason, we discretize the soil in  $n$  elementary disks (see Figure 3) . For the spatial discretization, we integrate Equation 4 over each disk  $k \in \llbracket 1, n \rrbracket$ . Divergence theorem leads to :

$$C_k \frac{\partial T_k}{\partial t} = R_{k-1}^{-1} (T_{k-1} - T_k) + R_k^{-1} (T_{k+1} - T_k). \quad (5)$$

The thermal lineic capacities and thermal resistances are calculated respectively with Equations 6 and 7.

$$C_1 = \pi \rho_s c_s \left( r_i + \frac{\delta r}{4} \right) \delta r \quad ; \quad C_k = 2\pi \rho_s c_s \left( r_i + (k-1)\delta r \right) \delta r \quad \text{for } k \geq 2 \quad (6)$$

$$R_k = \frac{\delta r}{2\pi \lambda_s \left( r_i + \left( k - \frac{1}{2} \right) \delta r \right)} \quad (7)$$

Equation 5 remains valid for  $k = 1$  by setting  $R_0 = R_i$ . Finally, we consider the thermal capacity of the pipe wall  $C_w = 2\pi \rho_p c_p r_p e_w$  and the resistance associated to convective

heat transfer between the fluid and the wall  $R_{fw}$ . Setting  $R_{-1} = R_{fw}$  and  $C_0 = C_w$ , the problem is reduced to the system of equations 5 for  $k \in \llbracket 0, n \rrbracket$  with the boundary conditions:

$$T_{-1} = T_f(t) \quad ; \quad T_{n+1} = T_g(t) \quad (8)$$

$T_f(t)$  is given by the network model (see section 2.4) and  $T_g(t)$  is the ground temperature undisturbed by the fluid at the depth of the pipe. For the latter, the model of Kusuda et al. [20] is used. The remaining ordinary differential equations are solved using the solver *odeint* from the *scipy* library [21]. Finally, we obtain the evolution of the lineic thermal losses  $\dot{Q}_{loss,f} = (T_0(t) - T_{-1}(t))/R_{-1}$ . Knowing the length of the pipes, the total heat losses along each pipe is computed and sent to the network model.

## 2.4 Iteration logic description

The principles of the iterative process between the different models are presented in Figure 4. The iteration proceeds from step (A) to (D). For steps (C) and (D), relaxation is implemented to smooth the convergence process (see Equation 9 for step D). For the initialization, the substation temperatures are set to default values while the edge losses are set to 0.

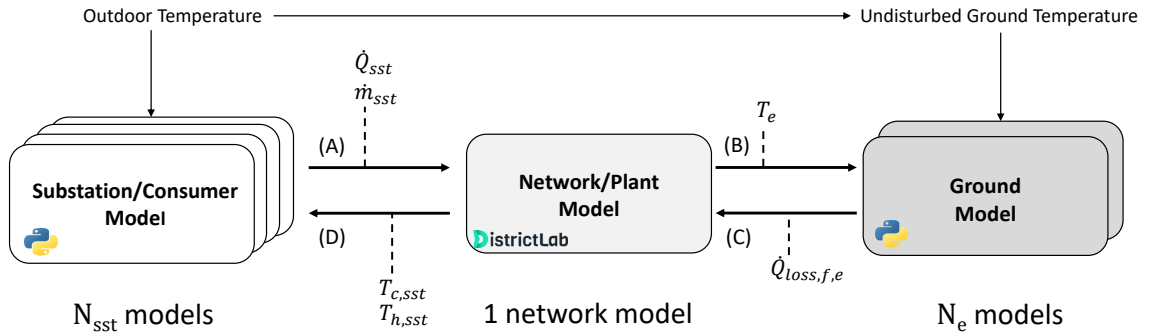


**Figure 4.** Description of the iterative process. One iteration consists in steps (A) to (D). At each step, there are multiple substation and ground models simulations. For the latter, a representative subset is chosen to reduce running time of simulation. The variables trajectories over the entire simulation period are exchanged between the different models.

The model of substation computes the mass flow rate that must cross each substation. The temperature entering the substation  $T_{in,SST}^S$  is determined by the network simulation. We define a relaxation parameter  $\alpha$  which characterizes the update of the temperature thanks to following equation :

$$T_{k+1}^S = \alpha T_k^N + (1 - \alpha) T_k^S, \quad (9)$$

where  $T_k^S$  is the input temperature of the substation simulation at iteration  $k$  and  $T_k^N$  is the output temperature of the network simulation at iteration  $k$ .  $\alpha$  takes value between 0 and 1.

The model of network takes as input the mass flow rate and heat exchange in each substation, and the thermal losses in each pipe. For each pipe, the model of soil takes the evolution of the fluid temperature in the pipe as input and gives the evolution of the thermal losses as output. The thermal losses are updated on a similar way as the equation 9. The output is a field of temperature in the network.



For each edge, the soil model takes the evolution of the fluid temperature as input and computes the evolution of the thermal losses.

### 3 Results

#### 3.1 Case study

As represented in Figure 5, the network is composed of 2 substations (offices and swimming pool) and a plant, balancing the energy of the network. We design the pipe diameter to limit both the pressure loss to 200 Pa/m and the velocity to 1.5 m/s.

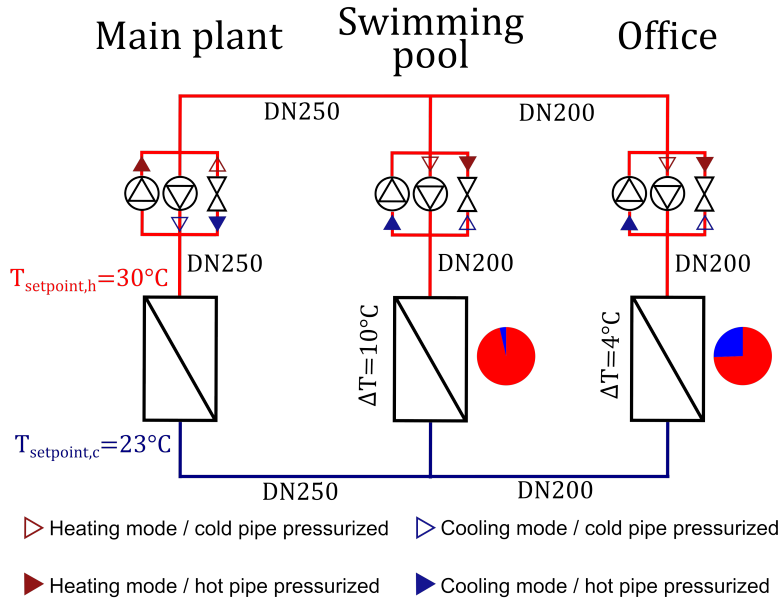


**Figure 5.** Case study with a main plant and two substations. The arrows are consistent with Figures 1 and 2. The pie charts represents the share of heating (red) and cooling (blue) demand over one year.

We set  $T_{setpoint,h} = 30^{\circ}C$  and  $T_{setpoint,c} = 23^{\circ}C$  for the plant. We assume that the main plant is fed for e.g. by water from a lake ( $10^{\circ}C$ ) and uses a i) a heat pump in case of overall heat demand and ii) a heat exchanger in case of overall cooling demand. We take  $\Delta T_{office} = 10^{\circ}C$  and  $\Delta T_{pool} = 4^{\circ}C$  as setpoint for the substation primary flow rate control.

We consider three representative periods of 15 days respectively in January, July and October. This corresponds to the 3 following cases: mainly hot demand, mainly cold demand, and quasi-balanced demand. The average hot and cold demand are represented on Table 2.

#### 3.2 Convergence analysis

In this section, we focus on the analysis of the convergence between the substation and network models. In a substation  $j$ , at the step time  $i$ , we define the gap  $g_j(i)$  and the overall gap with Equations 10 and 11 respectively.

**Table 2.** Average heat load over the three periods of 15 days considered.

	January		July		October	
	Heating demand (kWth)	Cooling demand (kWth)	Heating demand (kWth)	Cooling demand (kWth)	Heating demand (kWth)	Cooling demand (kWth)
Office	524	0	15	103	70	32
Swimming pool	330	0	41	10	76	3

$$g_j(i) = \max(\dot{m}_j(i), 0)^2 (T_{h,j}^S(i) - T_{h,j}^N(i))^2 + \min(\dot{m}_j(i), 0)^2 (T_{c,j}^S(i) - T_{c,j}^N(i))^2 \quad (10)$$

$$\text{gap} = c_P \sqrt{\frac{\sum_{j=1}^{N_{sst}} \sum_{i=1}^{n_{steps}} g_j(i)}{N_{sst} n_{steps}}} \quad (11)$$

The variable gap corresponds to the estimation of the average error in the calculation of the heat power entering each substation.  $\dot{m}_j(i)$  is the mass flow rate through substation  $j$  at time step  $i$ .  $T_{h,j}^N$  and  $T_{c,j}^N$  are the hot and cold temperature at the substation boundaries in the network simulation whereas  $T_{h,j}^S$  and  $T_{c,j}^S$  corresponds to the hot and cold temperature estimation in the substation model.  $c_P$  is the water heat capacity.  $N_{sst}$  is the number of substations whereas  $n_{steps}$  corresponds to the number of time step in the simulation.

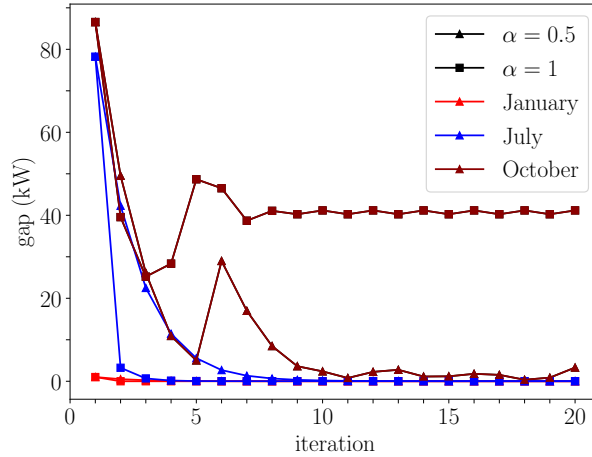


**Figure 6.** Evolution of the gap with the iterations. The shape of the marker is different for  $\alpha = 1$  (square) and  $\alpha = 0.5$  (triangle). The three different colors symbolize the three periods of simulation (January, July, October).

For each simulation, a time step of 5 minutes was considered and we performed 20 iterations. In Figure 6, we plot the evolution of the gap (equation 11) for  $\alpha = 0.5$  and  $\alpha = 1$ .

In January, the gap decreases towards zero, whatever the value of  $\alpha$ . With  $\alpha = 1$ , the convergence is faster.

In July, the gap does not tend towards zero. However, the values of the limit of the gap (17 W for  $\alpha = 0.5$  and 27 W for  $\alpha = 1$ ) can be neglected, regarding the average demand of 103 kW of cooling for the offices and 40 kW of heating for the swimming Pool (see Table 2). Finally, in October, the simulation does not converge (the limit of

the gap in one half of the demand) by taking  $\alpha = 1$ . Taking  $\alpha = 0.5$  leads to a minimal gap of 260 W, which is 0.4% of the average demand in each building. This analysis illustrates that the convergence process between the substation and the network model is rather stable. In general, a relaxation parameter of 0.5 and 10 iterations ensure a gap of less than 1%.

### 3.3 Pressure field analysis

As a preliminary results obtained with this model, we study the influence of the imposed pressure difference between the hot and the cold pipes and more specifically the sign of this minimal differential pressure. We define the configuration 'hot pipe pressurized' (HP) when the pressure of the hot pipe is at least 1 bar higher in all points of the network and the configuration 'cold pipe pressurized' (CP) inversely. The direction of the flow in the different configurations, i.e. *hot pipe pressurized* and *cold pipe pressurized* is shown in Figure 5. We focus on the electrical costs for the operation of the hydraulic pumps of the network, trying to find the most efficient configuration. Table 3 presents the consumption of the hydraulic pumps in the different simulations.

**Table 3.** Comparison of the sum of the electrical consumption of the hydraulic pumps in the network. The calculation of difference takes the first column as reference.

Month	Hot pipe pressurized (kWhe)	Cold pipe pressurized (kWhe)	Difference (%)
January	957.6	827.4	-13.6 (%)
July	118.6	116.8	-1.6 (%)
October	172.8	152.7	-11.6 (%)

In October and January, there is a significant difference between the two setups. In July, the consumption is similar for the 2 modes.

We first focus on the difference in January, where both substations need heat. We represent schematically the two configurations in Figure 7.

The pressure loss in the pipe between the main plant and the first substation (0-1) can be written using the Darcy-Weisbach formulation, as shown in Equation 12.

$$\Delta P_{0-1} = k_{0-1}(\dot{m}_1 + \dot{m}_2)^2 \quad (12)$$

The analytical expression of  $k_{0-1}$  is given in Equation 13, where  $D_{0-1}$  is the diameter of the pipe and  $L_{0-1}$  is its length.  $f_D$  is the Darcy friction factor.

$$k_{0-1} = \frac{8f_D L_{0-1}}{\rho \pi^2 D_h^5} \quad (13)$$

Similarly, the pressure loss between the two substations is :

$$\Delta P_{1-2} = k_{1-2} \dot{m}_2^2. \quad (14)$$

If the hot pipe is pressurized (HP), we use the centralized pump of the main plant (MP) :

$$P_{elec,HP} = \frac{1}{\eta_{MP}}(\dot{m}_1 + \dot{m}_2)\Delta P_{MP,HP}, \quad (15)$$

where  $\eta_{MP}$  is the electro-mechanical efficiency of the pump. We write the explicit form of  $\Delta P_{MP,HP}$ :

$$P_{elec,HP} = \frac{1}{\eta_{MP}}(\dot{m}_1 + \dot{m}_2)(\Delta P_{min} + 2k_{0-1}(\dot{m}_1 + \dot{m}_2)^2 + 2k_{1-2}\dot{m}_2^2). \quad (16)$$

$\Delta P_{min}$  is the minimal difference of pressure between the pressurized line and not pressurized line of the network. Staying above this threshold ensure that the design mass flow rate can flow through the substation and the main plant when the valves are fully open.

If the cold pipe is pressurized (CP), we use the decentralized pumps:

$$P_{elec,CP} = \frac{1}{\eta_{SST1}}\dot{m}_1\Delta P_{SST1,CP} + \frac{1}{\eta_{SST2}}\dot{m}_2\Delta P_{SST2,CP}. \quad (17)$$

We can explicit  $\Delta P_{SST1,CP}$  and  $\Delta P_{SST2,CP}$ :

$$P_{elec,CP} = \frac{1}{\eta_{SST1}}\dot{m}_1(\Delta P_{min} + 2k_{0-1}(\dot{m}_1 + \dot{m}_2)^2) + \frac{1}{\eta_{SST2}}\dot{m}_2(\Delta P_{min} + 2k_{0-1}(\dot{m}_1 + \dot{m}_2)^2 + 2k_{1-2}\dot{m}_2^2). \quad (18)$$

We assume that the three hydraulic pumps have the same efficiency  $\eta$ . The difference between the two configurations is then:

$$P_{elec,HP} - P_{elec,CP} = \frac{2}{\eta}k_{1-2}\dot{m}_1\dot{m}_2^2. \quad (19)$$

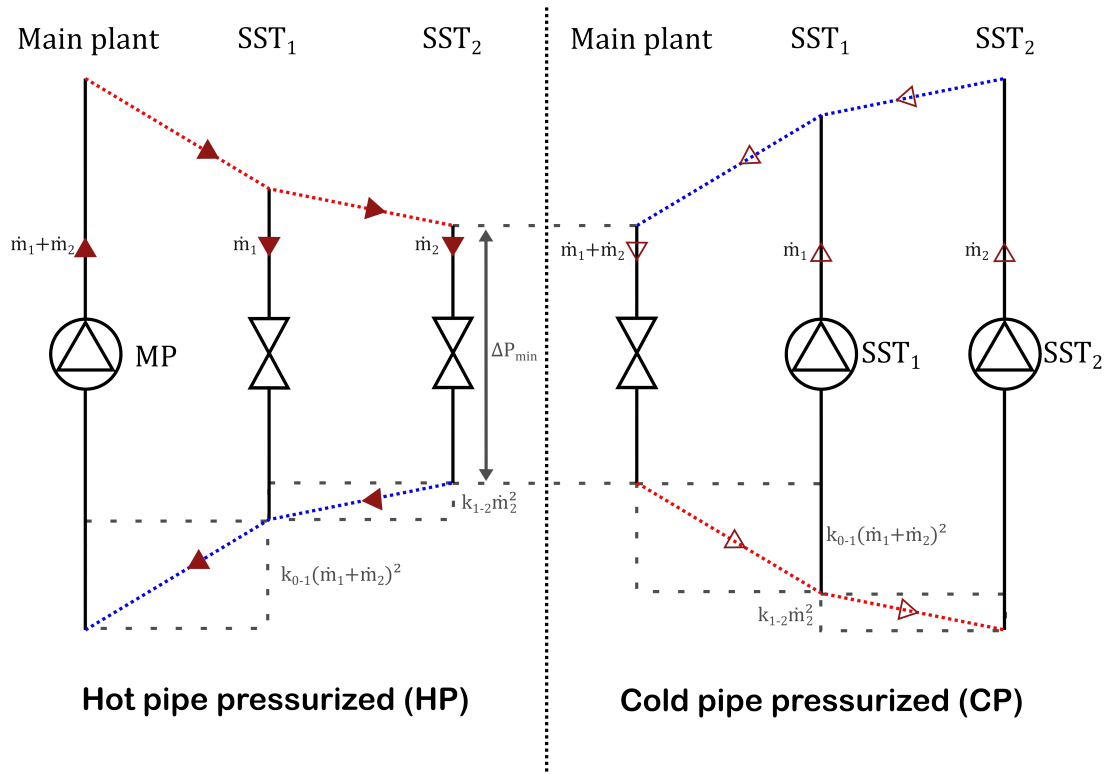


**Figure 7.** Pressure loss with both substations in heating mode. The left part presents the case of hot pipe pressurized and the right part presents the as of cold pipe pressurized. The arrows remind the notations of Figures 1, 2 and 5.

Equation 19 confirms what we observe on Table 3: It is more efficient to use the decentralized hydraulic pumps than a centralized pump. This difference is more sensible

to the mass flow through the most distant substation (quadratic relationship) than the other substation (linear relationship). In classical networks, such operation is unfeasible since there are only valves in substations, and the gain does not compensate the CAPEX of decentralized pumps. In bidirectional networks, where we need decentralized hydraulic pump to make the network bidirectional, the use of decentralized pumps in case of uniform demand leads to economical savings.

In July, where the cold demand dominates, one could expect the pressurization of the hot pipe to be the most efficient. Actually, there is still a need for heat in the swimming pool, and the higher value of  $\Delta T_{office}$  leads to a decrease of the mass flow rate through the office, that is the reason why the results are balanced. In October, the situation is a combination of both phenomena described for January and July.

## 4 Conclusion

In this paper, a versatile simulation solution for 5GDHC networks is introduced. It is based on an iterative process between 3 different models:

- A thermal model of substation,
- A thermal hydraulic model of primary network,
- A thermal resistive-capacitive model of soil.

The iteration between the different models allows taking into account the main physical phenomena involved in 5GDHC networks. In this paper, we have mainly studied the effects of the sign of the minimal imposed differential pressure between hot and cold pipes. Contrary to the current setup in classical network, it is here shown that it is more interesting to pressurize the cold pipe during winter and use decentralized hydraulic pumps in order to do so.

Thanks to the presented model, different scenarios will now be addressed. Especially, the sensitivity of the system performances depending on pipe insulation, balancing plant setpoint temperatures and difference of temperatures through each substation are on-going studies.

The latter will open the path to optimal control in order to determine the most favorable time-dependent thermal hydraulic conditions for the network's operation.

## Author contributions

CP collected the data, developed the model, performed the simulations and wrote the manuscript. NL supervised the project and reviewed the manuscript.

## Competing interests

The authors declare that they have no competing interests.

## Funding

This project has been financially supported by Institut Carnot " nergies du Futur".

## Acknowledgements

The authors wish to thank Roland BAVIERE and Julien RAMOUSSE, respectively from DistrictLab company and LOCIE Laboratory at USMB, for the many fruitful discussions we had during the development of the model.

## References

- [1] ADEME, “Développement des filières réseaux de chaleur et de froid renouvelables en France à horizon 2050,” Nov. 2020.
- [2] *The future of cooling*. <https://www.iea.org/reports/the-future-of-cooling>, Accessed: 2023-09-19, 2018.
- [3] S. Buffa, M. Cozzini, M. D’Antoni, M. Baratieri, and R. Fedrizzi, “5th generation district heating and cooling systems: A review of existing cases in Europe,” en, *Renewable and Sustainable Energy Reviews*, vol. 104, pp. 504–522, Apr. 2019, ISSN: 13640321. DOI: 10.1016/j.rser.2018.12.059. [Online]. Available: <https://linkinghub.elsevier.com/retrieve/pii/S1364032118308608> (visited on 04/11/2023).
- [4] T. Sommer, A. Sotnikov, M. Sulzer, et al., “Hydrothermal challenges in low-temperature networks with distributed heat pumps,” en, *Energy*, vol. 257, p. 124 527, Oct. 2022, ISSN: 03605442. DOI: 10.1016/j.energy.2022.124527. [Online]. Available: <https://linkinghub.elsevier.com/retrieve/pii/S036054422201430X> (visited on 04/11/2023).
- [5] K. Gjoka, B. Rismanchi, and R. H. Crawford, “Fifth-generation district heating and cooling systems: A review of recent advancements and implementation barriers,” en, *Renewable and Sustainable Energy Reviews*, vol. 171, p. 112 997, Jan. 2023, ISSN: 13640321. DOI: 10.1016/j.rser.2022.112997. [Online]. Available: <https://linkinghub.elsevier.com/retrieve/pii/S1364032122008784> (visited on 04/13/2023).
- [6] H. Hirsch and A. Nicolai, “An efficient numerical solution method for detailed modelling of large 5th generation district heating and cooling networks,” en, *Energy*, vol. 255, p. 124 485, Sep. 2022, ISSN: 03605442. DOI: 10.1016/j.energy.2022.124485. [Online]. Available: <https://linkinghub.elsevier.com/retrieve/pii/S0360544222013883> (visited on 05/24/2023).
- [7] M. Abugabbara, J. Lindhe, S. Javed, H. Bagge, and D. Johansson, “Modelica-based simulations of decentralised substations to support decarbonisation of district heating and cooling,” en, *Energy Reports*, vol. 7, pp. 465–472, Oct. 2021, ISSN: 23524847. DOI: 10.1016/j.egyr.2021.08.081. [Online]. Available: <https://linkinghub.elsevier.com/retrieve/pii/S2352484721006831> (visited on 04/11/2023).
- [8] R. Toffanin, P. Caputo, M. Belliardi, and V. Curti, “Low and Ultra-Low Temperature District Heating Equipped by Heat Pumps—An Analysis of the Best Operative Conditions for a Swiss Case Study,” en, *Energies*, vol. 15, no. 9, p. 3344, May 2022, ISSN: 1996-1073. DOI: 10.3390/en15093344. [Online]. Available: <https://www.mdpi.com/1996-1073/15/9/3344> (visited on 06/09/2023).
- [9] F. Bünning, M. Wetter, M. Fuchs, and D. Müller, “Bidirectional low temperature district energy systems with agent-based control: Performance comparison and operation optimization,” en, *Applied Energy*, vol. 209, pp. 502–515, Jan. 2018, ISSN: 03062619. DOI: 10.1016/j.apenergy.2017.10.072. [Online]. Available: <https://linkinghub.elsevier.com/retrieve/pii/S0306261917314940> (visited on 04/17/2023).
- [10] Y. Adihou, M. Kane, J. Ramousse, and B. Souyri, “An exergy-based district heating modeling for optimal thermo-hydraulic flow distribution: Application to bluefactory’s smart living lab neighborhood,” in *Proceedings of ECOS 2020-The 33rd International Conference*

- on Efficiency, Cost, Optimization, Simulation and Environmental Impact of Energy Systems, 29 June-3 July 2020, Osaka, Japan, 29 June-3 July 2020, 2020.*
- [11] A. Maccarini, A. Sotnikov, T. Sommer, M. Wetter, M. Sulzer, and A. Afshari, "Influence of building heat distribution temperatures on the energy performance and sizing of 5th generation district heating and cooling networks," en, *Energy*, vol. 275, p. 127 457, Jul. 2023, ISSN: 03605442. DOI: [10.1016/j.energy.2023.127457](https://doi.org/10.1016/j.energy.2023.127457). [Online]. Available: <https://linkinghub.elsevier.com/retrieve/pii/S0360544223008514> (visited on 09/07/2023).
  - [12] P. Saini, P. Huang, F. Fiedler, A. Volkova, and X. Zhang, "Techno-economic analysis of a 5th generation district heating system using thermo-hydraulic model: A multi-objective analysis for a case study in heating dominated climate," en, *Energy and Buildings*, vol. 296, p. 113 347, Oct. 2023, ISSN: 03787788. DOI: [10.1016/j.enbuild.2023.113347](https://doi.org/10.1016/j.enbuild.2023.113347). [Online]. Available: <https://linkinghub.elsevier.com/retrieve/pii/S0378778823005777> (visited on 08/24/2023).
  - [13] M. Wirtz, L. Kivilip, P. Remmen, and D. Müller, "5th Generation District Heating: A novel design approach based on mathematical optimization," en, *Applied Energy*, vol. 260, p. 114 158, Feb. 2020, ISSN: 03062619. DOI: [10.1016/j.apenergy.2019.114158](https://doi.org/10.1016/j.apenergy.2019.114158). [Online]. Available: <https://linkinghub.elsevier.com/retrieve/pii/S0306261919318458> (visited on 08/29/2023).
  - [14] M. Wirtz, "nPro: A web-based planning tool for designing district energy systems and thermal networks," en, *Energy*, vol. 268, p. 126 575, Apr. 2023, ISSN: 03605442. DOI: [10.1016/j.energy.2022.126575](https://doi.org/10.1016/j.energy.2022.126575). [Online]. Available: <https://linkinghub.elsevier.com/retrieve/pii/S0360544222034624> (visited on 04/17/2023).
  - [15] M. Wirtz, L. Kivilip, P. Remmen, and D. Müller, "Quantifying Demand Balancing in Bidirectional Low Temperature Networks," en, *Energy and Buildings*, vol. 224, p. 110 245, Oct. 2020, ISSN: 03787788. DOI: [10.1016/j.enbuild.2020.110245](https://doi.org/10.1016/j.enbuild.2020.110245). [Online]. Available: <https://linkinghub.elsevier.com/retrieve/pii/S0378778820309889> (visited on 04/13/2023).
  - [16] M. Abugabbara and J. Lindhe, "A Novel Method for Designing Fifth-Generation District Heating and Cooling Systems," en, *E3S Web of Conferences*, vol. 246, J. Kurnitski and M. Thalfeldt, Eds., p. 09 001, 2021, ISSN: 2267-1242. DOI: [10.1051/e3sconf/202124609001](https://doi.org/10.1051/e3sconf/202124609001). [Online]. Available: <https://www.e3s-conferences.org/10.1051/e3sconf/202124609001> (visited on 04/07/2023).
  - [17] *Districtlab, digital twin for energy grids*, <https://www.districtlab.eu/>.
  - [18] R. Baviere, M. Vallee, S. Crevon, N. Vasset, and N. Lamaison, "Districtlab-h: A new tool to optimize the design and operation of district heating and cooling networks," in *DHC Symposium 2023-The 18th International Symposium on District Heating and Cooling*, 2023.
  - [19] Y. Merlet, R. Baviere, and N. Vasset, "Optimal retrofit of district heating network to lower temperature levels," en, *Energy*, vol. 282, p. 128 386, Nov. 2023, ISSN: 03605442. DOI: [10.1016/j.energy.2023.128386](https://doi.org/10.1016/j.energy.2023.128386). [Online]. Available: <https://linkinghub.elsevier.com/retrieve/pii/S0360544223017802> (visited on 07/25/2023).
  - [20] T. Kusuda and P. R. Achenbach, *Earth temperature and thermal diffusivity at selected stations in the United States*. National Bureau of Standards Gaithersburg, MD, USA, 1965, vol. 71.
  - [21] P. Virtanen, R. Gommers, T. E. Oliphant, et al., "SciPy 1.0: Fundamental Algorithms for Scientific Computing in Python," *Nature Methods*, vol. 17, pp. 261–272, 2020. DOI: [10.1038/s41592-019-0686-2](https://doi.org/10.1038/s41592-019-0686-2).